Appl. Phys. B 60, 155–159 (1995)

Applied Physics B Lasers and Optics

An analytical model for evaporative cooling of atoms

K.B. Davis, M.-O. Mewes, W. Ketterle

Department of Physics and Research Laboratory of Electronics, Massachusetts Institute of Technology, Cambridge, MA 02139, USA
(Fax: +1-617/253-4876, E-mail: WOLFGANG@amo.mit.edu)

Received: 21 August 1994 / Accepted: 8 November 1994

Abstract. Evaporative cooling of trapped atoms is described as a sequence of truncation of the high-energy tail of the thermal distribution followed by collisional relaxation. This model is solved analytically for arbitrary power-law potentials. The threshold density for accelerated evaporation is found to be lowest in a three-dimensional linear potential.

PACS: 32.80.Ps; 42.50.Vk

Although laser cooling has seen rapid progress in the last few years it still has several severe limitations. There are absorption effects [1, 2] limiting the density of cold atoms, the recoil limit, and also heating and trap loss due to excited-state collisions. All of these limitations do not apply to evaporative cooling. In addition, atoms such as hydrogen which do not have convenient optical transitions can be evaporatively cooled. Until recently, evaporative cooling could only be applied to atomic hydrogen which can be pre-cooled by cryogenic methods [3–6]. Several groups are currently trying to extend evaporative cooling to laser-cooled atoms, and very recently two successful demonstrations were reported [7, 8].

Evaporative cooling was originally proposed by Hess [9]. It consists of the selective removal of atoms in the high-energy tail of the thermal distribution and the collisional equilibration of the remaining atoms. Although neither the selection of atoms nor collisions alone increase the phase-space density, the combination of both does [10]. It is even possible to simultaneously obtain a decrease in temperature and an increase in density if the shrinking volume of the atom cloud overcompensates for the loss in the number.

With reference to magnetically trapped hydrogen, several theoretical studies of evaporative cooling have been reported [11–15]. Some of these models included not only evaporative loss of atoms, but also dipolar relaxation [12–14] and three-body recombination [13, 14]. Presented here is a simplified analytical description including only elastic collisions, evaporative loss of particles and background gas collisions. One motivation for such a simple model is the fact that, for alkali atoms, the elastic cross section is roughly three orders of magnitude larger than for hydrogen. As a result, inelastic processes are negligible for a broad regime of temperatures and densities which is of interest for several experiments [7, 8]. A different analytical model for evaporation is discussed in [15] and could probably be applied to the situation discussed here.

The most important parameter to control the evaporation is the depth ηkT of the potential well. For small η, a large fraction of the atoms can escape over the threshold of the potential resulting in fast evaporation; however, the temperature reduction per escaping atom is small. It is this interplay between the truncation parameter η and the dynamics of the evaporation which is described in our model. In the most general situation, η will be varied with time to control and optimize the evaporation process. In this paper, we mainly study the effects of a single truncation step as a function of η.

Experiments on evaporation employ linear [7, 8] and harmonic [16] traps; the hydrogen work at MIT uses an anisotropic trap which can be regarded as a two-dimensional linear potential with steep walls providing confinement in the third dimension [3, 13]. The model presented here is valid for any number of dimensions and arbitrary power-law potentials. One rather unexpected result is that the important self-acceleration of evaporation is only pronounced in linear potentials.

1 The basic model

We model evaporative cooling as a discrete process. Truncation of the energy distribution at ηkT is followed by thermal relaxation in an infinitely deep potential resulting in a temperature decrease from the initial temperature T to T'. This cycle is repeated with an energy truncation of ηkT etc. In most experiments, the potential depth is lowered *continuously*, while the atoms stay in thermal equilibrium through elastic collisions. The discrete model has the advantage of having an exact solution can be used to study the basic interplay between the various parameters of the evaporation process.

Dedicated to H. Walther on the occasion of his 60th birthday

Table 1. During evaporative cooling, all relevant quantities scale as ν^x, where ν is proportional to the number of trapped particles

Quantity	Exponent x
Number of atoms N	1
Temperature T	γ
Volume V	$\xi\gamma$
Density n	$1-\xi\gamma$
Phase-space density γ	$1-\gamma(\xi+3/2)$
Elastic-collision rate nv	$1-\gamma(\xi-1/2)$

During one cycle, the number of trapped atoms is reduced from N to N'. It is convenient to express all important quantities as power laws ν^x with $\nu = N'/N$. Defining

$$\gamma = \frac{\log(T'/T)}{\log(N'/N)} , \tag{1}$$

the temperature changes as $T'/T = \nu^\gamma$ during one cycle. In a d-dimensional potential,

$$U(r) = \text{const. } r^m , \tag{2}$$

the volume occupied by the trapped atoms scales as $T^{d/m}$. This scaling arguments it independent on how the volume is defined (e.g., by a $1/e$ decay of the density, or as the number of atoms divided by peak density). Note that the potential in a spherical quadrupole magnetic trap is anisotropic, but it can be written in the form of (1) after a coordinate transformation $z' = 2z$.

For the density n, one obtains a power law

$$n'/n = \nu^{1-\xi\gamma} \tag{3}$$

with

$$\xi = d/m . \tag{4}$$

Since we are only interested in ratios n'/n, (3) holds for the peak density as well as the average density. Power laws exist for all other quantities (Table 1).

If j discrete evaporation steps are performed, ν has to be substituted by ν^j. The dynamics of evaporation is entirely described by the two quantities ν and γ.

These two quantities are calculated for an arbitrary power-law potential r^m in d dimensions from integrals involving the density of states $D(E)$

$$D(E) = \frac{(2M)^{3/2}}{\hbar^3(2\pi)^2} \int_{V(E)} \sqrt{E - \text{const. } r^m}\, \mathrm{d}^3 r . \tag{5}$$

$V(E)$ is the available position space for particles with energy E and atomic mass M [17]. Note that we are always considering a *three*-dimensional gas confined in d dimensions (either unconfined in the remaining 3-d dimensions or confined by infinitely steep walls).

The occupation number of classical particles in an energy level E in the trap is $\exp[-(E-\mu)/kT]$. Effects of quantum statistics can be neglected for a dilute gas. The fraction ν of particles with energy E smaller than ηkT is

$$\nu(\eta) = \frac{1}{N} \int_0^{\eta kT} D(E) \mathrm{e}^{-(E-\mu)/kT} \mathrm{d}E . \tag{6}$$

The chemical potential μ is determined by the normalization $\nu(\infty) = N$.

Introducing the normalized energy $\varepsilon = E/kT$ and $\sigma(\varepsilon) = (kT/N)D(\varepsilon kT)\mathrm{e}^{\mu/kT}$ as the normalized density of states, one obtains

$$\nu(\eta) = \int_0^\eta \sigma(\varepsilon)\mathrm{e}^{-\varepsilon}\mathrm{d}\varepsilon , \tag{7}$$

with

$$\sigma(\varepsilon) = \frac{\varepsilon^{1/2+\xi}}{\Gamma(3/2+\xi)} . \tag{8}$$

Note that the chemical potential and the constants in (4) are both absorbed in the normalization factor in (6). The integral in (5) can be solved in terms of generalized gamma functions which are reduced for specific values of ξ to the expressions shown in Table 2.

The function $\gamma(\eta)$ is obtained from the total energy $\alpha(\eta)NkT$ of the trapped atoms after truncation

$$\alpha(\eta) = \int_0^\eta \varepsilon\sigma(\varepsilon)\mathrm{e}^{-\varepsilon}\mathrm{d}\varepsilon . \tag{9}$$

The average total energy per atom in units of kT is $\alpha(\eta)/\nu(\eta)$.

For $\eta \to \infty$, one obtains

$$\alpha(\infty) = (3/2) + \xi . \tag{10}$$

$\alpha(\eta)$ can be obtained in analytical form (Table 2). The normalized energy per atom after re-thermalization gives the decrease in temperature from T to T' per evaporation cycle

$$\frac{T'}{T} = \frac{\alpha(\eta)}{\nu(\eta)\alpha(\infty)} . \tag{11}$$

From (1), one obtains

$$\gamma = \frac{\log\left(\frac{\alpha(\eta)}{\nu(\eta)\alpha(\infty)}\right)}{\log[\nu(\eta)]} . \tag{12}$$

The average energy of an evaporated atom is $\varepsilon_{\text{eff}}\, kT$, with

$$\varepsilon_{\text{eff}} = \frac{\alpha(\infty) - \alpha(\eta)}{1-\nu(\eta)} , \tag{13}$$

or equivalently,

$$\varepsilon_{\text{eff}} = \left(\xi + \frac{3}{2}\right) \frac{1-\nu(\eta)^{\gamma(\eta)+1}}{1-\nu(\eta)} . \tag{14}$$

For a large cutoff parameter η, $\nu(\eta) \to 1$. Expanding (10b) by treating $1-\nu(\eta)$ as a small parameter, yields

$$\gamma = \frac{\varepsilon_{\text{eff}}}{(3/2)+\xi} - 1 . \tag{15}$$

Therefore, for large η, γ is a dimensionless quantity characterizing how much more than the average energy is removed by the evaporated atoms. A similar equation was used by Hess [(4) in [9]] including magnetic decompression and losses due to dipolar relaxation. For large truncation parameters η, one can integrate (10a) by parts and obtains $\varepsilon_{\text{eff}} \to \eta + 1$, implying $\gamma \to \infty$. The temperature reduction per evaporated atom is large, but the evaporation process is slow because there are only few a with energy larger than ηkT.

For small η, one obtains from (5), (7) and (9), $\gamma = 2/(3+2\xi)$. On first sight, it is surprising that the increase in phase-space density has its maximum for $\eta \to 0$ (Fig. 2). However,

Table 2. The evaporation process in a d-dimensional potential r^m is described by two characteristic functions $\alpha(\eta)$ and $\nu(\eta)$ which depend only on $\xi = d/m$

ξ	$\nu(\eta)$	$\alpha(\eta)$
3/2	$1 - \frac{2+2\eta+\eta^2}{2e^\eta}$	$3 - \frac{6+6\eta+3\eta^2+\eta^3}{2e^\eta}$
2	$\frac{-2\sqrt{\eta}(15+10\eta+4\eta^2)}{15e^\eta\sqrt{\pi}} + \mathrm{erf}(\sqrt{\eta})$	$\frac{-\sqrt{\eta}(105+70\eta+28\eta^2+8\eta^3)}{15e^\eta\sqrt{\pi}} + \frac{7\,\mathrm{erf}(\sqrt{\eta})}{2}$
3	$\frac{-2\sqrt{\eta}(105+70\eta+28\eta^2+8\eta^3)}{105\,e^\eta\sqrt{\pi}} + \mathrm{erf}(\sqrt{\eta})$	$\frac{-\sqrt{\eta}(945+630\eta+252\eta^2+72\eta^3+16\eta^4)}{105\,e^\eta\sqrt{\pi}} + \frac{9\,\mathrm{erf}(\sqrt{\eta})}{2}$

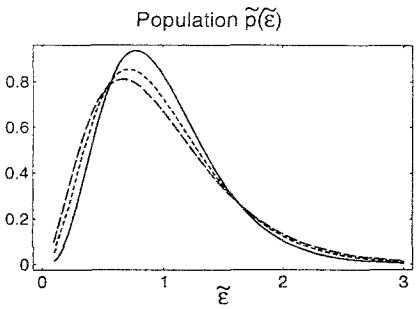

Fig. 1. Population of energy levels $\tilde{p}(\tilde{\varepsilon})$ (12). The *short dashed*, *dashed* and *solid curves* are for $\xi = 3/2$ (3-dim. harmonic potential), $\xi = 2$ (2-dim. linear potential), $\xi = 3$ (3-dim. linear potential)

this corresponds to the selection of the energy levels with the largest population. After thermalization, the lowest levels have even larger population corresponding to an increase in phase-space density [10].

2 Comparison for different potentials

In the following discussion, we examine evaporation in different trap geometries. Notice that, for this purpose, it is more natural to measure energies not in units of kT, but rather in units of the average total energy $(3/2 + \xi)kT$. We denote energies and truncation parameters normalized in this way by $\tilde{\varepsilon}$ and $\tilde{\eta}$, respectively, i.e.,

$$\tilde{\varepsilon} = \frac{\varepsilon}{\frac{3}{2} + \xi} \,. \tag{16}$$

The normalized density of occupied states,

$$\tilde{p}(\tilde{\varepsilon}) = \sigma(\varepsilon)\left(\frac{3}{2} + \xi\right) \mathrm{e}^{-\varepsilon} \,, \tag{17}$$

(normalized in such a way that $\int_0^\infty \tilde{p}(\tilde{\varepsilon})\mathrm{d}\tilde{\varepsilon} = 1$) is similar for different trap geometries having a peak centered around the average energy (normalized to 1) with a width of approximately 1 (Fig. 1). It is, therefore, not surprising that the functions ν and γ are similar too, or in other words, the decrease in atom number and in temperature is similar for different potentials when the energy truncation is performed at the same $\tilde{\eta}$. This conclusion is not valid at very small or large $\tilde{\eta}$, but these regions are of minor practical interest for evaporative cooling.

In contrast, the density increase is much larger for large ξ since the volume of the trapped sample scales with temperature as T^ξ. Similarly, the changes in phase-space density ρ and elastic-collision rate strongly depend on the potential parameter ξ (Fig. 2). (The elastic collision rate is given by $n\sigma_{\mathrm{el}}v$, where σ_{el} denotes the elastic collision cross section and v the atom velocity.) In current experiments with laser-cooled atoms, the initial density is just sufficient to start the evaporative-cooling process because the thermalization time (which is inversely proportional to the elastic-collision rate) is comparable to the trapping time. Significant evaporative cooling probably requires a speed-up in the thermalization rate. This means that the cloud has to be truncated at sufficiently large η or γ. Indeed, from Table 1, one obtains the inequality

$$\gamma > \frac{1}{\xi - 1/2} \tag{18}$$

for accelerated collision rates. For larger potential parameters ξ, evaporation at smaller γ is favorable (Fig. 2). Indeed, for a three-dimensional linear potential ($\xi = 3$), the largest increase in the thermalization rate is found at $\tilde{\eta} = 0.8$. At such values of $\tilde{\eta}$, a parabolic trap ($\xi = 3/2$) would already exhibit a decrease of the thermalization rate. Evaporation at such small $\tilde{\eta}$ values is accompanied by a substantial loss of trapped particles. Experiments employing this strategy might eventually be limited by the sensitivity of probing very few atoms.

3 Inclusion of background-gas collisions

So far, we have not taken into account loss of atoms due to background-gas collisions. If the trapping time is t_{trap}, and one evaporation cycle is carried out in a time interval t_{step}, the number of particles is reduced by an additional factor $\exp(1/\tau)$ during this cycle with

$$\tau = t_{\mathrm{trap}}/t_{\mathrm{step}} \,. \tag{19}$$

We can incorporate this loss process by considering one evaporation cycle as consisting of three steps: truncation at η, rethermalization, loss of particles by a factor $\exp(1/\tau)$. We could incorporate this additional loss in the number of atoms into the exponents in Table 1, as was done by Hess for the γ exponent [9]. However, an equivalent approach chosen here is to calculate all quantities without trap loss and then multiply N, n, ρ and nv by $\exp(1/\tau)$ and leave T and V unchanged.

Snoke and collaborators have shown that the energy distribution is almost indistinguishable from the equilibrium distribution after five collisions [18, 19]. τ is then approximately one fifth of the ratio between the elastic-collision rate and the trap-loss collision rate which is colloquially called the ratio of good-to-bad collisions.

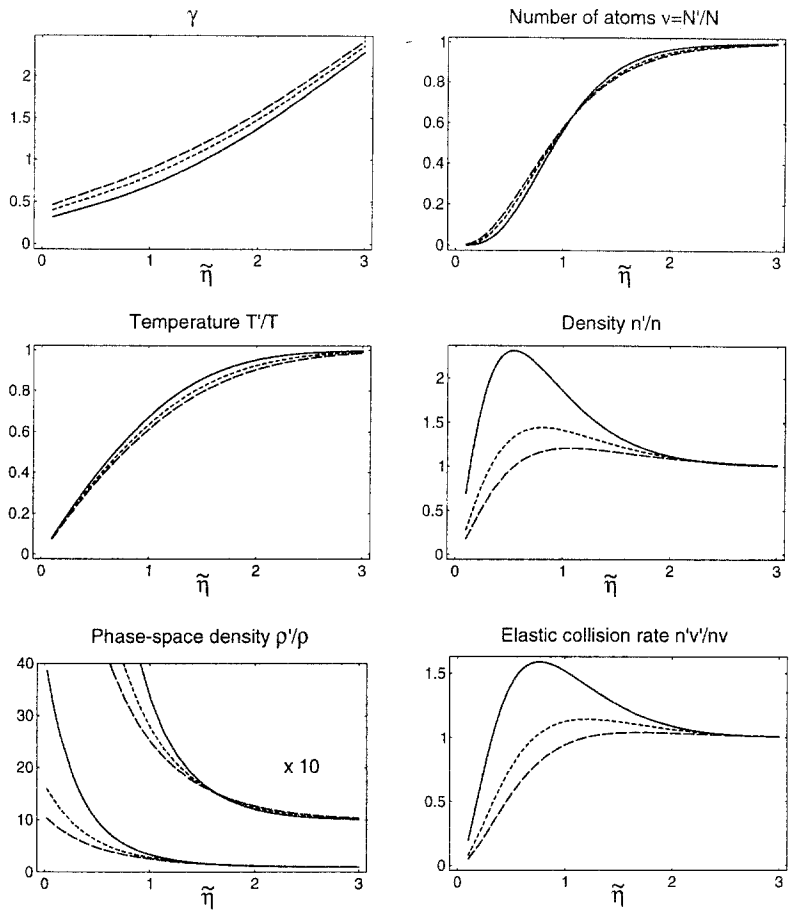

Fig. 2. Dependence of various quantities during evaporation on the truncation parameter $\tilde{\eta}$. The *short dashed*, *dashed* and *solid curves* are for $\xi = 3/2$ (3-dim. harmonic potential), $\xi = 2$ (2-dim. linear potential), $\xi = 3$ (3-dim. linear potential). The first graph shows the temperature exponent γ, the others the ratios of various quantities after and before a single truncation/thermalization step

In the absence of trap loss, the maximum increase in the thermalization rate is 1.04 for a parabolic potential and 1.59 for a three-dimensional linear potential (Fig. 2). This big difference is a consequence of the more pronounced shrinking of the cloud with temperature for large ξ which, furthermore, allows evaporation to be carried out at smaller truncation parameters $\tilde{\eta}$. Figures 3a, c show the increase in the thermalization rate for several values of τ. Accelerated evaporation requires a minimum value of τ which is 2.2 for the three-dimensional linear potential and 24 for the parabolic case, more than an order of magnitude higher. This means that accelerated evaporation in a parabolic trap requires a considerably higher initial density or lower residual-gas pressure than in a spherical quadrupole trap. However, a parabolic trap with a very small bias field (e.g., a Ioffe trap) has a linear potential in the two transverse directions except for a small region at the bottom which is rounded off. If the atom cloud extends well beyond the parabolic region, the trap can be regarded as a linear trap in two dimensions and a parabolic trap in the third dimension, corresponding to $\xi = 5/2$ (see [17] for the derivation of the density of states for traps with different power laws of the potential in different dimensions). Such a field configuration would avoid trap loss due to Majorana flops at the zero of the magnetic field, and simultaneously provide tight-enough confinement for accelerated evaporation.

A more refined model should account for the change in the elastic-collision rate during thermalization. Immediately after truncation the rate is smaller than before truncation by approximately a factor $N'v'/Nv = \nu^{1+\gamma/2}$. This reduction shifts the optimum strategy to larger values of $\tilde{\eta}$. In a worst-case model, we assume that the elastic-collision rate during a thermalization step is constant and equal to the rate immediately after truncation. The number τ of truncation/thermalization steps during one trapping time is then dependent on $\tilde{\eta}$ through

$$\tau = \tau_0 \nu^{1+\gamma/2} , \tag{20}$$

where τ_0 is inversely proportional to the thermalization time before truncation.

We find the minimum τ_0 for accelerated evaporation to be 4.7 for the spherical quadrupole trap and 29 for the parabolic trap. The latter value corresponds to roughly 150 elastic collisions per trapping time, in agreement with the same value obtained in [16] from Monte-Carlo simulations. The threshold for accelerated evaporation in a spherical quadrupole trap should be as low as approximately 25 elastic collisions per atom and trapping time.

With (14), the optimum increase in phase-space density no longer happens for $\eta \to 0$. The long thermalization time after a deep truncation results in increased loss of atoms due to background-gas collisions and favors truncation at larger η. Optimized strategies for multi-step evaporation require additional study. For instance, if the overall goal is to maximize phase-space density, it could be more advantageous to focus first on increased thermalization rate and then to maximize phase-space density when fast thermalization times prevent excessive loss of atoms due to background-gas collisions. However, one possible simple strategy is obvious without further elaboration: if the initial conditions for accelerated evaporation are met and η is kept in the range for increased collision rates, density and phase-space density will contin-

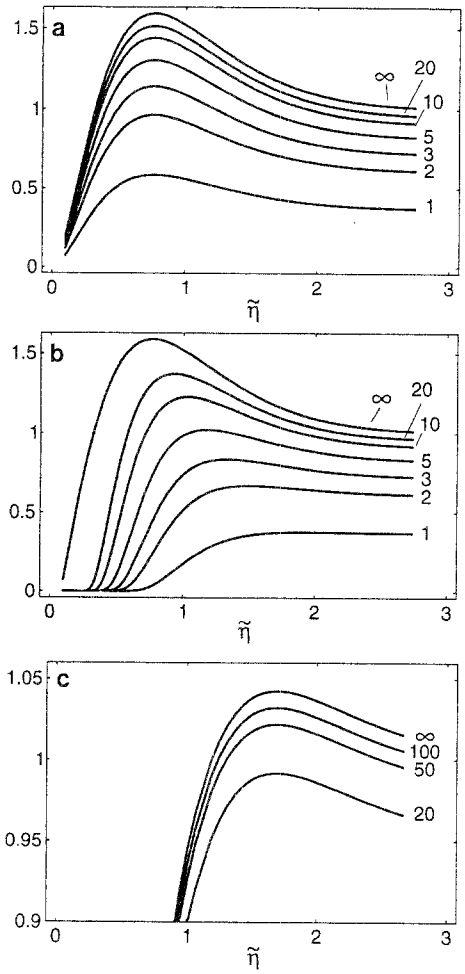

Fig. 3a–c. Relative change in the elastic collision rate vs truncation parameter $\tilde{\eta}$; **(a)** 3-dim. linear potential ($\xi = 3$), the different trapping times are characterized by the values of τ (13) given in the figure; **(b)** same as **(a)**, but using τ_0 as parameter (14); **(c)** same as **(a)**, but for a 3-dim. harmonic potential ($\xi = 3/2$)

uously increase. Ultimately, this increase is limited by loss processes (dipolar relaxation and three-body recombination) which are neglected in the model discussed here.

4 Conclusions

In conclusion, we have presented a simple formalism to treat evaporative cooling of trapped atoms. This formalism provides guidance to optimize forced evaporation (i.e., variation of the potential depth with time). Different strategies maximize the increase in density, phase-space density or thermalization rate. An important prediction is that the threshold density for accelerated evaporation is considerably higher in a parabolic trap than in a spherical quadrupole trap.

Acknowledgements. This work was supported by the Office of Naval Research and Air Force Office of Scientific Research through grant N00014-90-J-1642, the Joint Services Electronics Program and the Sloan Foundation. M.-O.M. and K.B.D. would like to acknowledge support from Studienstiftung des Deutschen Volkes and the M.I.T. Physics Department Lester Wolfe fellowship, respectively.

References

1. D.W. Sesko, T.G. Walker, C.E. Wieman: J. Opt. Soc. Am. B **8**, 946 (1991)
2. W. Ketterle, K.B. Davis, M.A. Joffe, A. Martin, D.E. Pritchard: Phys. Rev. Lett. **70**, 2253 (1993)
3. N. Masuhara, J.M. Doyle, J.C. Sandberg, D. Kleppner, T.J. Greytak, H.F. Hess, G.P. Kochanski: Phys. Rev. Lett. **61**, 935 (1988)
4. J.M. Doyle, J.C. Sandberg, I.A. Yu, C.L. Cesar, D. Kleppner, T.J. Greytak: Phys. Rev. Lett. **67**, 603 (1991)
5. O.J. Luiten, H.G.C. Werij, I.D. Setija, M.W. Reynolds, T.W. Hijmans, J.T.M. Walraven: Phys. Rev. Lett. **70**, 544 (1993)
6. I.D. Setija, H.G.C. Werij, O.J. Luiten, M.W. Reynolds, T.W. Hijmans, J.T.M. Walraven: Phys. Rev. Lett. **70**, 2257 (1993)
7. W. Petrich, M.H. Anderson, J.R. Ensher, E.A. Cornell: *14th Int'l Conf. on Atomic Physics*, Boulder, CO (1994) Book of Abstracts, 1M-7
8. K.B. Davis, M.O. Mewes, M.A. Joffe, W. Ketterle: *14th Int'l Conf. on Atomic Physics*, Boulder, CO (1994) Book of Abstracts, 1-M3
9. H.F. Hess: Phys. Rev. B **34**, 3476 (1986)
10. W. Ketterle, D.E. Pritchard: Phys. Rev. A **46**, 4051 (1992)
11. R.V.E. Lovelace, C. Mahanian, T.J. Tommila, D.M. Lee: Nature **318**, 30 (1985)
12. T. Tommila: Europhys. Lett. **2**, 789 (1986)
13. J.M. Doyle: Energy distribution measurements of magnetically trapped spin polarized atomic hydrogen: Evaporative cooling and surface sticking. Ph.D. thesis, Massachusetts Institute of Technology, Cambridge, MA (1991)
14. J.M. Doyle, J.C. Sandberg, I.A. Yu, C.L. Cesar, D. Kleppner, T.J. Greytag: Physica B **194-196**, 13 (1994)
15. O.J. Luiten: Lyman-alpha spectroscopy of magnetically trapped atomic hydrogen. Dissertation, University of Amsterdam (1993)
16. C.R. Monroe, E.A. Cornell, C.A. Sackett, C.J. Myatt, C.E. Wieman: Phys. Rev. Lett. **70**, 414 (1993)
17. V. Bagnato, D.E. Pritchard, D. Kleppner: Phys. Rev. A **35**, 4354 (1987)
18. D.W. Snoke, J.P. Wolfe: Phys. Rev. B **39**, 4030 (1989)
19. D.W. Snoke, W.W. Ruehle, Y.-C. Lu, E. Bauser: Phys. Rev. B **45**, 10979 (1992)